J Electr Eng Technol Vol. 9, No. 4: 1277-1282, 2014
http://dx.doi.org/10.5370/JEET.2014.9.4.1277

ISSN(Print) 1975-0102
ISSN(Online) 2093-7423

Efficiency Improvement for Concentrated Flux IPM Motors for Washing Machines

Keun-young Yoon* and Byung-il Kwon†

Abstract – Concentrated flux interior permanent magnet (CFIPM) motors have the advantage that their utilization of flux linkage is more efficient than that of general IPM motors and CFIPM motors are suitable for washing machine motors, which demand low-speed, high-torque specifications. However, low efficiency occurs in the low-speed high-torque mode considering the high-speed operation for spin mode. This paper proposes a magnet overhang structure between the rotor core that reduces leakage flux and improves efficiency for a CFIPM in wash mode. Optimization of the 3D design of magnet overhang structures is performed to improve the efficiency with the same quantity of permanent magnets. The validity of the optimal design is experimentally verified through the fabrication of prototypes.

Keywords: Concentrated flux, Efficiency, Leakage flux, Magnet overhang, Optimal design

1. Introduction

Recently in the washing machine market, there has been increased in requests for large washing capacity and high efficiency. To accomplish this, motor design focuses on washing machine motors that will improve power-density and high efficiency.

The operation of a washing machine motor is divided into two modes. One is wash mode, with low-speed and high-torque, and the other is spin mode, with high-speed and low-torque. Therefore a washing machine motor should be designed to take the characteristics of both these different operating modes into account. Compared to the high-speed mode, the low-speed, high-torque mode has a relatively low efficiency. In addition, the recent demand for larger washing capacity increases the load torque in the wash mode, ensuring that the wash mode has low efficiency and low out-power. The price limit of the washing machine is constrained by the price of the washing machine motor, which in turn limits the quality of raw material that can be used for the motor. In most cases, only aluminum wires and ferrite magnets can be used. With these materials, it is difficult to improve efficiency in the wash mode with its low-speed and high-torque. Therefore, the shape of the washing machine motor must be chosen to improve the power density and efficiency.

The inductances of the d-axis and q-axis of interior permanent magnet (IPM) motors are different. Thus, IPM motors can use the reluctance torque in addition to the magnet torque [1, 2]. Thus the entire torque of these motors is higher than that of surface permanent magnet (SPM) motors, which only use the magnet torque. Accordingly, IPM motors have been extensively researched for systems requiring high power density and high efficiency [3].

Concentrated flux IPM (CFIPM) motors have a different rotor structure that can concentrate the flux, compared to conventional IPM motors. In CFIPM motors, the amount of useful flux linkage can be maximized. Therefore, the efficiency and the power density of CFIPM motors can be improved [4-7] and CFIPM motors should be suitable for the wash mode of a washing machine

To increase the power density of CFIPM motors for a washing machine, the number of poles should be increased. However, poles may have large leakages because they are close to the distance between the rotor cores, and the rotor core size is smaller than that of a structure with a low pole number. This reduces the efficiency of the wash mode.

This study proposes a magnet overhang structure between the rotor core and the magnet that reduces leakage flux and improves the efficiency of the wash mode. The magnet overhang structure means that the magnet height is greater than the rotor core height. Furthermore with design optimization of the magnet overhang structure, we maximize the efficiency of the CFIPM motor [10, 11]. The optimization variables are the dimensions of the magnet and rotor core. We use two optimization approaches: the Kriging model based on Latin hypercube sampling (LHS) and a genetic algorithm (GA) [12-15]. The optimal results from the optimization algorithm are verified with 3D-finite element analysis (FEA). To confirm the analysis and the optimal design results, the optimal model has been manufactured and tested.

† Corresponding Author: Dept. of Electronic Systems Engineering, Hanyang University, Korea. (bikwon@hanyang.ac.kr)
* Dept. of Mechatronics Engineering, Hanyang University, Korea. (azure@hangyang.ac.kr)
Received: May 18, 2013; Accepted: January 22, 2014

2. CFIPM Motor

2.1 Configuration and specification

Home appliances such as the washing machine use multi-polar structured CFIPM motors, which can be modeled with inner-rotor-type structures and concentrated-winding-type stators. Fig. 1 shows a CFIPM motor, where the permanent magnet has been magnetized in a concentrated flux direction.

The specifications of the CFIPM motor are listed in Table 1. The stator and the rotor have an overhang, so that the stator is longer than the rotor cores. However the lengths of the rotor core and magnet are the same. In this study, overhang structures are not applied to the model.

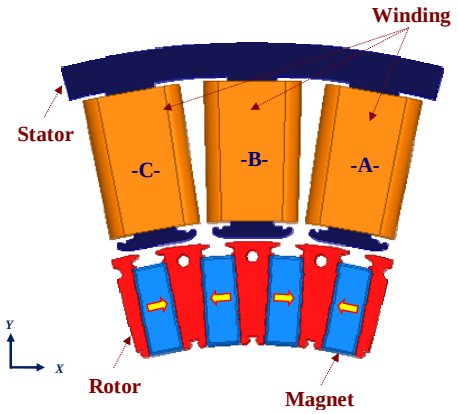

Fig. 1. Structure of the CFIPM motor

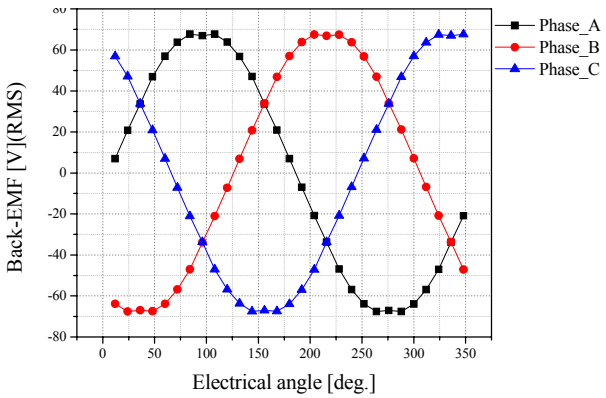

Fig. 2. Back-EMF of a basic model (at 150 rpm)

Table 1. Specification of basic model

Item	Unit	Value
Pole / Slot No.	-	48 / 36
Stator height	mm	23
Rotor height	mm	29
Magnet height	mm	29
Stator Out-diameter	mm	304.0
Stator Inner-diameter	mm	225.0
Rotor Out-diameter	mm	223.2
Residual flux density	T	0.42
Air-gap	mm	0.9

Fig. 2 shows the back-electromotive force (Back-EMF) of the basic model, which is 45.62 Vrms.

2.2 Proposed magnet overhang

In terms of the effective flux linkage, CFIPM motors have an advantage because the rotor cores and magnets are arranged to concentrate the flux structure. As the number of poles increases, the distances between magnets and rotor cores as well as their sizes decrease, which then cause the leakage flux to increase. Leakage fluxes in concentrated flux structures with high pole numbers have various paths. A major leakage flux path exists on the upper and lower sides, as shown in Fig. 3(a). These leakage fluxes reduce the efficiency. To reduce the leakage flux, we propose a magnet overhang on the rotor core, as shown in Fig. 3(b).

A magnet overhang is applied as a rotor core that is 1 mm longer than the fixed-height magnet on both the upper and lower sides, as shown in Fig. 3(b). To confirm the effect of the overhang, the leakage flux is calculated for Region 1, shown in Fig. 3(b), both in the cases of no overhang and a 1mm overhang. As shown in Table 2, the leakage flux decreased by 12.3%, due to the magnet overhang between the magnet and rotor core. This shows the relationship between magnet overhang and leakage flux. Therefore, the heights of the magnet and rotor core are established as optimization design variables to determine the optimal size for the magnet overhang.

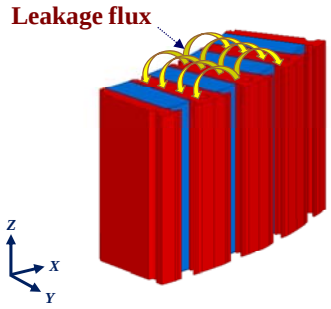

(a) No magnet overhang (Upper flux leakage is large)

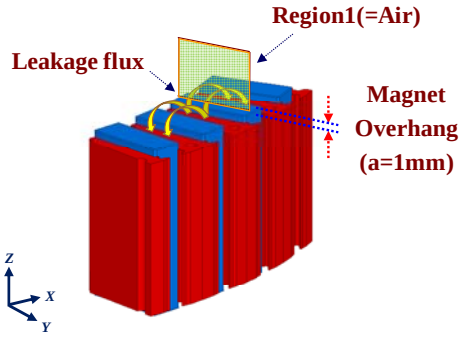

(b) Magnet overhang (Upper flux leakage is small)

Fig. 3. Leakage flux by overhang structure

Table 2. Characteristics of magnetic overhang

Item	Unit	No magnet overhang	Magnet overhang
Magnet overhang	mm	0	1
Leakage flux	Wb* e^{-5}	1.0905	0.9567 (12.3% ↓)
Back-EMF	Vrms	45.62	46.21
Efficiency	%	41.5	42.3

3. Optimal Design

3.1 Optimal design of the CFIPM motor

A flow chart of the optimization strategy is shown in Fig. 4. First, objective functions and constraints are defined. Then, sampling points is established in accordance with the design of experiment (DOE). Next, the approximation modeling is performed using the Kriging technique and the GA. Finally, the optimal values of the design variables are obtained.

The Kriging model has stronger linearity than the traditional response surface method (RSM) and thus accurate approximation modeling functions of nonlinear data can be obtained using this model. In addition, to improve the accuracy of the Kriging model that is highly dependent on data, the Latin hypercube sampling (LHS) technique is used as a DOE [16, 17]. The LHS makes experimental points into a matrix consisting of n lines and k columns and arranges individual lines as experimental points where n is the number of levels and k is the number of design variables. In particular, the characteristics of the LHS are that when creating design points, overlapping between experimental points and that the LHS can be easily implemented [18].

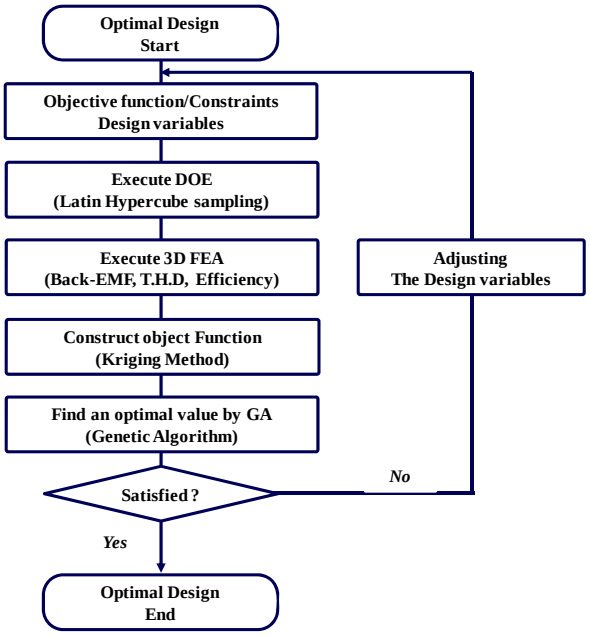

Fig. 4. Optimization process

3.2 Objective functions, constrains and design variables

The objective function is the maximum efficiency. The RMS value and the total harmonic distortion (T.H.D) characteristic of Back-EMF are established as constraints so that the operating characteristics would not be lower than those of the basic model. The weights of the rotor cores and magnets which are closely related to the material costs are established as constraints.

• ***Objective function:***

Maximize: Efficiency

$$f(x) = \frac{P_{out}}{P_{out} + P_{Copperloss} + P_{Ironloss}}$$

• ***Constraints:***

Back-EMF (RMS) > 46.0Vrms, T.H.D < 3.15%
Rotor cores weight < 1.5kg
Magnet weight = 0.875kg

The design variables for optimization are shown in Fig. 5. The height of the stator is fixed at 23 mm and the number of permanent magnets is specified as that of the basic model. Design variables are established to determine the optimal point of the overhang structure at which leakage flux would be minimized. Design variable X1 is the height of the rotor core, X2 is the height of each permanent magnet, X3 is the length of each permanent magnet, and X4 is the width of each permanent magnet. Since the same volume of permanent magnets is used, the height of the magnet (X2) is determined based on X3 and X4. Since the combinations of the design variables determine the physical distances of leakage flux that occur between the rotor core and the magnet, the optimal design point, where the leakage flux is minimized, can be determined.

The ranges of the design variables for the optimal design are as follows:

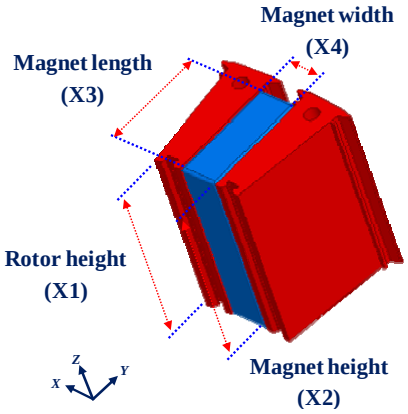

Fig. 5. Optimization process

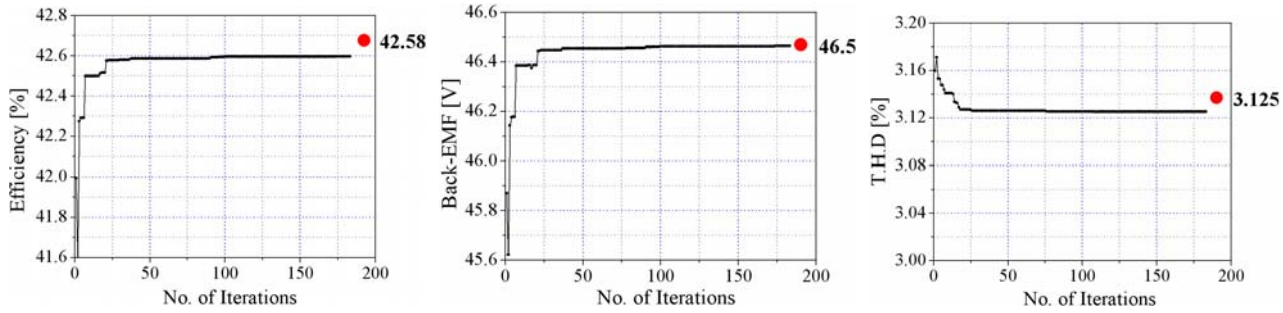

(a) (b) (c)

Fig. 6. Convergence progress of the subject function

Table 3. The analysis results for each variable by DOE

X1 [mm]	X2 [mm]	X3 [mm]	X4 [mm]	Efficiency [%]
27.00	16.90	7.30	29.60	45.89
29.00	17.40	7.10	29.60	45.65
25.00	16.30	7.70	29.10	44.79
26.00	19.70	6.30	29.40	46.40
26.00	17.10	7.90	27.00	44.02
28.00	16.60	7.00	31.40	45.95
28.00	17.70	7.40	27.90	45.33
26.00	18.00	7.00	29.00	46.33
23.00	18.00	6.40	31.70	44.79
24.00	19.10	6.90	27.70	46.18
25.00	18.60	6.00	32.70	45.48
26.00	16.00	7.60	30.00	45.28
27.00	19.40	6.10	30.90	46.29
23.00	18.30	6.70	29.80	45.37
24.00	18.90	7.60	25.40	46.12

Table 4. Characteristics of the basic model and optimal model

Item	Unit	Basic model (Analysis)	Optimal model (Analysis)
Rated torque	Nm	28	28
Phase current	A	3.21	3.14
Copper loss	W	186.21	178.23
Iron loss	W	20.48	17.82
Output power	W	146.61	146.63
Efficiency	%	41.5	42.8
Back-EMF	Vrms	45.62	46.63
Rotor weight	kg	1.05	1.47
Magnet Weight	kg	0.877	0.876

• ***Design variables:***

X1 (Rotor height): 23 mm < X1 < 29 mm
X2 (Magnet height): 25 mm < X2 < 32 mm
X3 (Magnet length): 16 mm < X3 < 20 mm
X4 (Magnet width): 6 mm < X4 < 8 mm

3.3 Optimal design results

To maximize the efficiency, design variables are established as X1, X2, X3, and X4. As shown in Table 3, the analysis results for each variable by DOE show the relationship between design variables and the objective function.

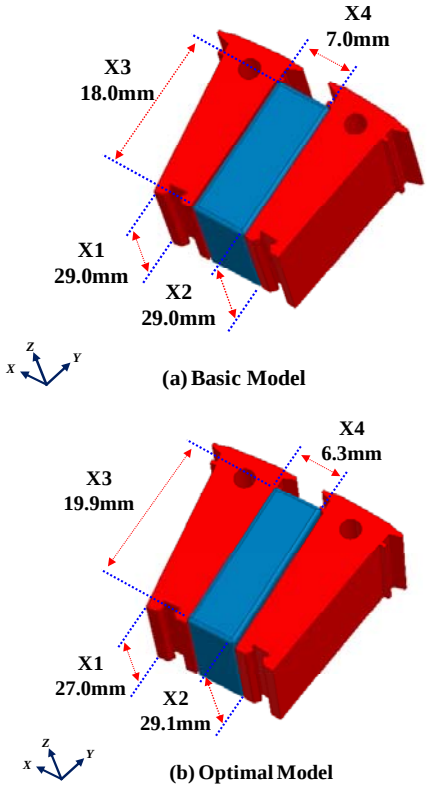

Design variable	Unit	Basic model	Optimal model
X1	mm	29.0	27.0
X2	mm	29.0	29.1
X3	mm	18.0	19.9
X4	Mm	7.0	6.3

Fig. 7. Dimensions of the basic model and optimal model

Using the GA, we determined an optimal design point that satisfied both the objective function and the constraints. Fig. 6 shows the convergence of the objective function and constraints using the GA. The individual design variables converged on an optimal design point.

The optimal values of the design variables are calculated by the convergence processes, as shown in Fig. 7.

The analysis results of the 3D characteristics of the optimal model are shown in Table 4. The Back-EMF is improved over the basic model by 2.2%, and the phase

current is decreased, thus the efficiency is improved from 41.5% to 42.8%, whereas the normal range of efficiency of a washing machine is 30-40% due to the washing mechanism. These results show that the leakage flux is reduced and the amount of flux linked to the stator is increased. In addition, the T.H.D is improved by 1.5%.

4. Experiment

The validity of the optimal design is verified through fabricating and experimenting on the prototype. Fig. 8 shows a prototype of the optimized CFIPM motor.

Fig. 8. The optimized CFIPM motor

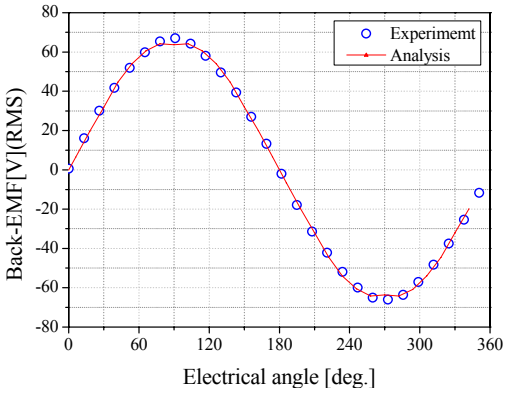

Fig. 9. Back-EMF of the prototype (at 150 rpm)

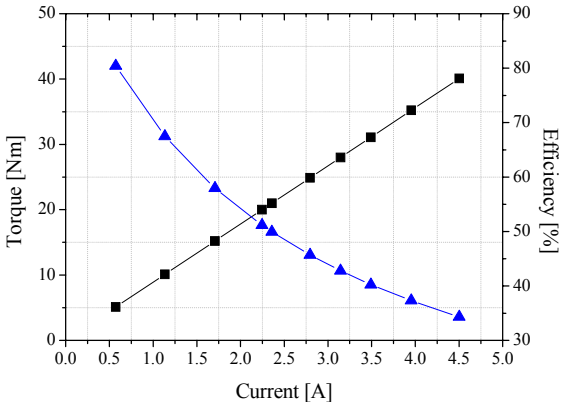

Fig. 10. Torque-Efficiency curve of the prototype

Table 5. Analysis and experiment results of optimal model

Item	Unit	Optimal model (Analysis)	Prototype (Experiment)
Rated torque	Nm	28	28
Phase current	A	3.14	3.10
Copper loss	W	178.23	173.27
Iron loss	W	17.82	17.33
Output power	W	146.61	146.67
Back-EMF	Vrms	46.63	46.64
Efficiency	%	42.8	43.5

The Back-EMF of the optimal prototype model is shown in Fig. 9 and Fig. 10 shows the torque-efficiency curve at wash mode. As shown in Table 5, the experimental results of the prototype confirmed the analysis results of the characteristics in the optimal model.

5. Conclusion

In this paper, we proposed a magnet overhang structure to reduce leakage flux and consequently improve the efficiency of CFIPM motors with high pole numbers. Optimization of the 3D design is performed and as shown in Table 6. The result showed improvement of the Back-EMF by 2.2% over the basic model, with a 2.0 point improvement in efficiency. In addition, by fabricating and experimenting with the prototype model, we confirmed that the actual efficiency is improved.

Table 6. Comparison of the basic and prototype model

Item	Unit	Basic model	Prototype model
Back-EMF	Vrms	45.62	46.64 (2.2% ↑)
Efficiency	%	41.5	43.5 (2.0point ↑)

Acknowledgement

This research was supported by BK21PLUS program through the National Research Foundation of Korea funded by the Ministry of Education.

References

[1] J.R. Hendershot, Jr. and T.J.E. Miller, Design of Brushless Permanent Magnet Motor. Oxford, U.K.: Clarendon, 1994.

[2] L. Fang et al., “Study on High-Efficiency Performance in Interior Permanent-Magnet Synchronous Motor With Double-layer PM Design,” IEEE Trans. on Magnetics, Vol. 44, pp. 4393-4396, November 2008.

[3] B.J. Chalmers et al., “Performance of Interior Type Permanent Magnet Alternator,” Proc. Inst. Elect. Eng., Elect. Power, Vol. 141, pp. 186-190, January 1994.

[4] Lin. D et al., "Analytical Prediction of Cogging Torque for Spoke Type Permanent Magnet Machine," IEEE Trans. on Magnetics, Vol. 48, pp. 1035-1038, February 2012.
[5] K.H. Yim et al., "Forced Vibration Analysis of an IPM Motor for Electrical Vehicles due to Magnetic Force," IEEE Trans. on Magnetics, Vol. 48, pp. 2981-2984, November 2012.
[6] Rukmi Dutta et al., "Design and Analysis of an Interior Permanent Magnet (IPM) Machine With Very Wide Constant Power Operation Range," IEEE Trans. Energy Conversion, vol. 23, pp. 25-33, March 2008.
[7] K.Y. Hwang et al., "A Study on Optimal Pole Design of Spoke-Type IPMSM With Concentrated Winding for Reducing the Torque Ripple by Experiment Design Method," IEEE Trans. on Magnetics, Vol. 45, pp. 4712-4715, October 2009.
[8] K.C. Kim et al., "The Study on the Overhang Coefficient for Permanent Magnet Machine by Experiment Design Method," IEEE Trans. on Magnetics, Vol. 43, pp. 1833-1836, April 2006.
[9] K. C. Kim et al., "The Dynamic Analysis of Spoke-Type Permanent Magnet with Large Overhang," IEEE Trans. on Magnetics, Vol. 41, pp. 3805-3808, October 2005.
[10] T. Ohnishi et al., "Optimal Design of Efficient IPM Motor Using Finite Element Method," IEEE Trans. on Magnetics, Vol. 36, pp. 3537-3539, September 2000.
[11] A. Koski et al., "Predicting The Performance of a Permanent Magnet Synchronous Motor by Analytical and Numerical Methods," IEEE Trans. on Magnetics, Vol. 28, pp. 935-938, January 1992.
[12] T. W. Simpson et al., "Kriging Models for Global Approximation in Simulation-Based Multidisciplinary Design Optimization," AIAA, Vol. 39, pp. 2233-2241, 2001.
[13] M. Lukaniszyn, et al., "Optimization of Permanent Magnet Shape for Minimum Cogging Torque Using a Genetic Algorithm," IEEE Trans. on Magnetics, Vol. 40, No. 2, March 2004.
[14] Hany M. Masanien, et al., "Design Optimization of Transverse Flux Linear Motor for Wight Reduction and Performance Improvement Using Response Surface Methodology and Genetic Algorithms," IEEE. Trans. on Energy Convers. Vol. 25, No. 3, September 2010.
[15] Uler. G. F, et al., "Utilizing genetic algorithms for the optimal design of electromagnetic devices," IEEE, Trans. on Magnetics, Vol. 30, No. 6, pp. 4296-4298, November 1994.
[16] K.Y. Hwang et al., "Rotor Pole Design in Spoke Type BLDC Motor by RSM," IEEE, Trans. on Magnetics, Vol. 45, pp. 4712-4715, October 2009.
[17] Y. Zhang et al., "Shape optimization of a PMLSM using Kriging and genetic algorithm," ICIEA, Vol. 45, pp. 1496-1499, 2010.
[18] Luiz Lebensztajn, et al., "Kriging: A Useful Tool for Electromagnetic Device Optimization," IEEE Trans. Magnetics, Vol. 40, No. 2, March 2004.

Byung-Il Kwon He received his B.S. and M.S. degrees in Electrical Engineering from Hanyang University, Korea and his Ph.D. in Electrical Engineering from Tokyo University, Japan. He is currently a Professor at Hanyang University. His research interests are linear drive systems, numerical analysis of electric machines and motor control.

Keun-Young Yoon He received his B.S. and M.S. degrees in Electronics Engineering from Hanyang University in 2003 and 2005. He is currently an Engineer at Samsung Electronics.